

## INFLUENCE OF THE ATMOSPHERIC TURBULENCE OUTER SCALE ON THE VARIANCE OF A LASER BEAM GRAVITY CENTER SHIFTS

V.P. Kandidov, M.P. Tamarov, and S.A. Shlyonov

*M.V. Lomonosov State University, Moscow*

*International Laser Center*

*Received April 29, 1997*

*Wandering and turbulent broadening of a laser beam is studied by the Monte Carlo method. Phase screens constructed by the modified subharmonic method are used to simulate atmospheric turbulence. The outer scale of atmospheric turbulence reproduced by a phase screen is estimated. The results of statistical experiments for propagation of collimated and focused laser beams are compared with the analytical estimates and data of field experiments.*

Large-scale spatial inhomogeneities of the air refractive index cause wandering of a beam as a whole. Efficiency and reliability of optical systems significantly depend on fluctuations in the direction of radiation propagation, so the study of this effect is of great practical importance.

At present, the Monte Carlo method (MCM) based on the phase screen model (PSM)<sup>1</sup> is a widely spread technique in the theoretical study of wave propagation in randomly inhomogeneous media. The method is most developed in papers on optics of turbulent atmosphere. This approach is used to study strong intensity fluctuations of a plane wave,<sup>2,3</sup> bounded light beams,<sup>4</sup> spatial statistics of a powerful laser radiation in the atmosphere,<sup>5</sup> and adaptive optics.<sup>6-8</sup>

According to the PSM, laser beam propagation is considered as a process of its sequential passing through a set of phase screens simulating random perturbations of the wave front by fluctuations in the refractive index of a continuous medium. So, numerical formation of the phase screens with a given fluctuation statistics is the key problem of such studies.

To form a phase screen, one usually uses the spectral method<sup>9</sup> or, less frequently, the method of moving summation.<sup>10</sup> According to the spectral method, the random phase  $\tilde{\varphi}(x, y)$  is calculated by filtration of the Gaussian pseudorandom field  $\tilde{\eta}(x, y)$ . The transfer function of the filter is defined by spatial spectrum of phase fluctuations  $F_{\varphi}(\kappa_{\perp})$  where  $\kappa_{\perp}$  is the frequency of the transverse spectral components of the phase  $\tilde{\varphi}(x, y)$ . According to the method of moving summation,  $\tilde{\varphi}(x, y)$  is determined by summation of the field  $\tilde{\eta}(x, y)$ , with the weights related to  $F_{\varphi}(\kappa_{\perp})$ , being shifted along the numerical grid. In these methods, the largest spatial scale of phase fluctuations is close to the grid cell size  $A = N \cdot h$ ,

where  $N$  is the number of the grid nodes,  $h$  is the grid step. So they are not applicable to the study of beam wandering in the atmosphere.

According to the modal approach, the phase is formed as a superposition of Zernike modes.<sup>11</sup> In the modal method, the formation of the screen phase begins from large-scale fluctuations, whereas in the spectral method it begins from small-scale ones. So, if the dimension of the array of basic functions (i.e., Zernike modes in the modal method or Fourier harmonics in the spectral method) is bounded, the modal method adequately reproduces large-scale phase fluctuations, while the spectral method and method of moving summation reproduce small-scale fluctuations.<sup>12</sup> Using these methods for generating phase screens to be applied to the problems of turbulent atmosphere optics imposes significant restrictions upon the range of spatial scale of the atmospheric inhomogeneities.

The possibility of constructing the phase screen in a wide range of atmospheric fluctuation scales on the basis of combination of the spectral and modal methods was discussed in Ref. 13.

To widen the range of the spectral method applicability to large-scale fluctuations, the algorithm of imbedded grids and the subharmonic method are proposed in Ref. 14 and Ref. 15, respectively. Modification of the methods<sup>16</sup> significantly improves the reproduction accuracy for low-frequency spatial fluctuations on a phase screen.

In this paper, we study wandering and turbulent broadening of a laser beam by MCM in which, to simulate the atmospheric turbulence, phase screens constructed by the modified subharmonic method are used. The outer scale of the atmospheric turbulence reproduced by a phase screen is estimated. The results of statistical experiments for propagation of collimated and focused laser beams are compared with the analytical estimates and data of field experiments.

### PHASE SCREEN

The spectrum of phase fluctuations on a screen is set by the expression

$$F_{\varphi}(\boldsymbol{\kappa}_{\perp}) = 2\pi k^2 \Delta z \Phi_n(\boldsymbol{\kappa}_{\perp}, 0), \quad \boldsymbol{\kappa}_{\perp}^2 = \kappa_x^2 + \kappa_y^2, \quad (1)$$

where  $\Delta z$  is the thickness of the turbulent layer replaced by the phase screen. The contribution of large-scale atmospheric perturbations determining the beam wandering along the path is described using von Karman model for the spatial fluctuation spectrum of the refractive index,  $\Phi_n(\boldsymbol{\kappa}_{\perp}; \boldsymbol{\kappa}_z)$

$$t_n(\boldsymbol{\kappa}_{\perp}, \boldsymbol{\kappa}_z) = 0.033 C_n^2 (\boldsymbol{\kappa}^2 + \boldsymbol{\kappa}_0^2)^{-11/6}; \quad \boldsymbol{\kappa}^2 = \boldsymbol{\kappa}_{\perp}^2 + \boldsymbol{\kappa}_z^2, \quad \boldsymbol{\kappa}_0^2 = (2\pi/L_0)^2, \quad (2)$$

where  $L_0$  is the outer scale of the atmospheric turbulence.

Random phase values for the light field of a beam are reproduced on a numerical grid in the plane  $XOY$  perpendicular to the propagation direction. For the isotropic turbulence, it is natural to take a square grid with the step  $h$  and aperture  $A$  along the axes  $x$  and  $y$ .

According to the spectral method, the algorithm of the phase  $\tilde{\varphi}(n, m)$  formation on the grid is as follows:

$$\begin{aligned} \tilde{\varphi}(n, m) &= \\ &= \frac{1}{N} \sum_{p=-(N/2)+1}^{(N/2)} \sum_{q=-(N/2)+1}^{(N/2)} a_{pq} (\tilde{\xi}_{pq} + i\tilde{\eta}_{pq}) W_N^p W_N^q; \\ a_{pq} &= \sqrt{F_{\varphi}(p, q)} \Delta \boldsymbol{\kappa}; \quad W_N = \exp\{i 2\pi/N\}; \\ F_{\varphi}(p, q) &= F(\Delta \boldsymbol{\kappa} p, \Delta \boldsymbol{\kappa} q), \end{aligned} \quad (3)$$

where  $\tilde{\xi}_{pq}, \tilde{\eta}_{pq}$  are the statistically independent random numbers distributed according to the Gaussian law  $(0, 1)$ ;  $\Delta \boldsymbol{\kappa} = 2\pi/A$  is the spectral interval between harmonics of the discrete spatial phase spectrum  $F_{\varphi}(p, q)$ ;  $N = A/h$  is the number of the grid nodes along the  $x$  and  $y$  axes. The real and imaginary parts of the complex phase  $\tilde{\varphi}(n, m)$  yield two statistically independent fields with the spatial spectrum  $F_{\varphi}(p, q)$ .

In the problem considered, the coefficient  $a_{00}$  is assumed to be zero because the zero harmonic  $\boldsymbol{\kappa}_{00}$  in the spectrum  $F_{\varphi}(p, q)$  represents the mean phase shift on the screen. The shift does not influence statistical properties of radiation. In the plane  $\boldsymbol{\kappa}_x, \boldsymbol{\kappa}_y$ , the vector of lowest frequency  $(p, q = \pm 1)$  of the spatial spectrum  $\boldsymbol{\kappa}_{11}$  is defined by the coordinates

$$\boldsymbol{\kappa}_{11} = (\pm \Delta \boldsymbol{\kappa}, \pm \Delta \boldsymbol{\kappa}). \quad (4)$$

High calculation efficiency which can be reached using the FFT algorithm is an advantage of the spectral method. False correlation arising at the scale  $l \geq A/2$

for the field  $\tilde{\varphi}(n, m)$  is its shortcoming. So, the method does not permit one to form fields whose largest correlation scale does not exceed  $A/2$ . For the Karman spectrum of atmospheric turbulence, the applicability of the spectral method is conditioned by the following expression for the outer scale  $L_0$ :

$$L_0 < A/2. \quad (5)$$

At the same time, reproduction of small-scale distortions in the beam profile is possible if the step  $h$  is much less than the beam radius  $a_0$ :

$$h \ll a_0. \quad (6)$$

Since usually  $a_0 \ll L_0$ , simultaneous fulfillment of the conditions (5) and (6) in a numerical experiment imposes significant restrictions on the range of spatial scales of atmospheric fluctuations.

In the subharmonic methods,<sup>16</sup> the spatial scale of phase fluctuations is wider in the low-frequency range. The resulting field is represented as a sum of the high-frequency part  $\tilde{\varphi}_{\text{hf}}$  obtained using usual spectral method and the low-frequency part  $\tilde{\varphi}_{\text{lf}}$  formed by subharmonics:

$$\tilde{\varphi}(n, m) = \tilde{\varphi}_{\text{hf}}(n, m) + \tilde{\varphi}_{\text{lf}}(n, m). \quad (7)$$

To obtain  $\tilde{\varphi}_{\text{lf}}$ , the spectral range near the zero harmonic is divided into several subharmonics.

In the modified subharmonic method,<sup>16</sup> the low frequency part of the phase field is formed in accordance with the algorithm

$$\begin{aligned} \tilde{\varphi}_{\text{lf}}(n, m) &= \frac{1}{N} \sum_{j=1}^{N_j} \sum_{p'=-3}^2 \sum_{q'=-3}^2 a_{p'q'} (\tilde{\xi}_{jp'q'} + i\tilde{\eta}_{jp'q'}) \times \\ &\times \exp \left[ 2\pi i 3^{-j} \left( \frac{(p'+0.5)}{N} + \frac{(q'+0.5)}{N} \right) \right]; \end{aligned} \quad (8)$$

$$a_{p'q'} = 3^{-j} \sqrt{F_{\varphi}(\boldsymbol{\kappa}'_x, \boldsymbol{\kappa}'_y) \Delta \boldsymbol{\kappa}_x \Delta \boldsymbol{\kappa}_y},$$

where  $N_j$  is the number of subharmonic iterations.

At each  $j$ th iteration, the phase spectrum is completed with  $3^j$  harmonics for which the spatial frequency vector  $\boldsymbol{\kappa}$ , in the plane  $\boldsymbol{\kappa}_x, \boldsymbol{\kappa}_y$ , is determined by the coordinates

$$\begin{aligned} \boldsymbol{\kappa}'_x &= 3^{-j} (p' + 0.5) \Delta \boldsymbol{\kappa}_x, \\ \boldsymbol{\kappa}'_y &= 3^{-j} (q' + 0.5) \Delta \boldsymbol{\kappa}_y. \end{aligned} \quad (9)$$

The subharmonics  $F_{\varphi}(\boldsymbol{\kappa}'_x, \boldsymbol{\kappa}'_y)$  with the indices  $(p', q')$  equal to  $(0, 0)$ ,  $(-1, -1)$ ,  $(0, -1)$ , and  $(-1, 0)$  are assumed to be zero. Since the spectral ranges of subharmonics and main spectral components overlap, one introduces weight factors for the main harmonics with the indices  $(p, q)$  equal to  $(\pm 1, 0)$ ,  $(0, \pm 1)$ , and

$(\pm 1, \pm 1)$  in order to keep the variance of the screen phase constant.

To analyze correlation properties of fields obtained by the modified subharmonic method, we have performed a numerical experiment in which the correlation function of the screen phase is calculated by the Monte Carlo method

$$B_{\phi}^{\text{Num}}(\rho_{lk}) = B_{\phi}^{\text{Num}}(\sqrt{l^2 + k^2} h) = \frac{1}{M(N-l)(N-k)} \times \sum_{i=1}^M \sum_{m=1}^{N-lN-k} \tilde{\varphi}^{(i)}(m, n) \tilde{\varphi}^{*(i)}(m+l, n+k), \quad (10)$$

where  $M$  is the number of field realizations. We used a square grid with the size  $A = 51.2 \text{ cm}$   $512 \times 512$  nodes. The field was generated by the spectral method and modified subharmonic method with the number of iterations  $j = 2, 4$ . Large number of iterations for grids of such a size requires too long computer time. We considered a field with the Karman spectrum (2) with the structure constant  $C_n^2 = 5 \cdot 10^{-15} \text{ cm}^{-2/3}$ . In generating the phase screen, three different values of the outer turbulence scale were used,  $L_0^{\text{appr}} = 0.5 \text{ m}$ ,  $5 \text{ m}$ , and  $50 \text{ m}$ .

Correlation functions  $B_{\phi}^{\text{Num}}$  obtained numerically are presented in Figs. 1a and b for several *a priori* values of  $L_0^{\text{appr}}$ . One can see that, if  $L_0^{\text{appr}} \leq A/2$ , the number of iterations  $N_j$  in the subharmonic method influences  $B_{\phi}^{\text{Num}}$  only insignificantly. However, if  $L_0^{\text{appr}} > A/2$ , the function  $B_{\phi}^{\text{Num}}$  and the position of the function with respect to the axis of ordinates, and, consequently, the variance  $\sigma_{\phi}^2$  significantly vary with increasing  $N_j$ . This follows from the fact that the outer scale  $L_0$  for the screen phase field obtained in the numerical experiment varies with increasing  $N_j$ .

The outer scale  $L_0$  for the phase screen formed by the subharmonic method was determined as the parameter such that the function  $B_{\phi}^{\text{Num}}$  obtained by the Monte-Carlo method is most closely approximated by the analytical expression for the screen correlation function  $B_{\phi}(\rho)$  and the field (2). Analytically, the correlation phase function on the screen for Karman spectrum (2) with the outer scale  $L_0$  has the form

$$B_{\phi}(\rho) = \sigma_{\phi}^2 \frac{2^{1/6}}{\Gamma(5/6)} (\alpha_0 \rho)^{5/6} K_{5/6}(\alpha_0 \rho), \quad (11)$$

where  $\Gamma(-)$  is the gamma function;  $K(-)$  is the McDonald function. The variance of the phase fluctuations is equal to

$$\sigma_{\phi}^2 = 2.4\pi^2 k^2 \Delta z \cdot 0.033 C_n^2 \alpha_0^{-5/3}. \quad (12)$$

Since periodicity is characteristic of the fields obtained by spectral methods, the deviation

$(B_{\phi}^{\text{Num}} - B_{\phi})^2$  was minimized for  $\rho \in [0, A/2]$ . Figure 1 presents some results of approximating the function  $B_{\phi}^{\text{Num}}$  obtained using MCM by the analytical expression  $B_{\phi}(\rho)$  depending on the parameter  $L_0$ . The approximation was performed by the least squares method. Analysis demonstrates that satisfactory approximation of  $B_{\phi}^{\text{Num}}$  by  $B_{\phi}(\rho)$  is reached with the iteration number  $N_j$  such that the obtained value of the outer scale  $L_0$  is close to the *a priori*  $L_0^{\text{appr}}$  (see the fragment in Fig. 1b).

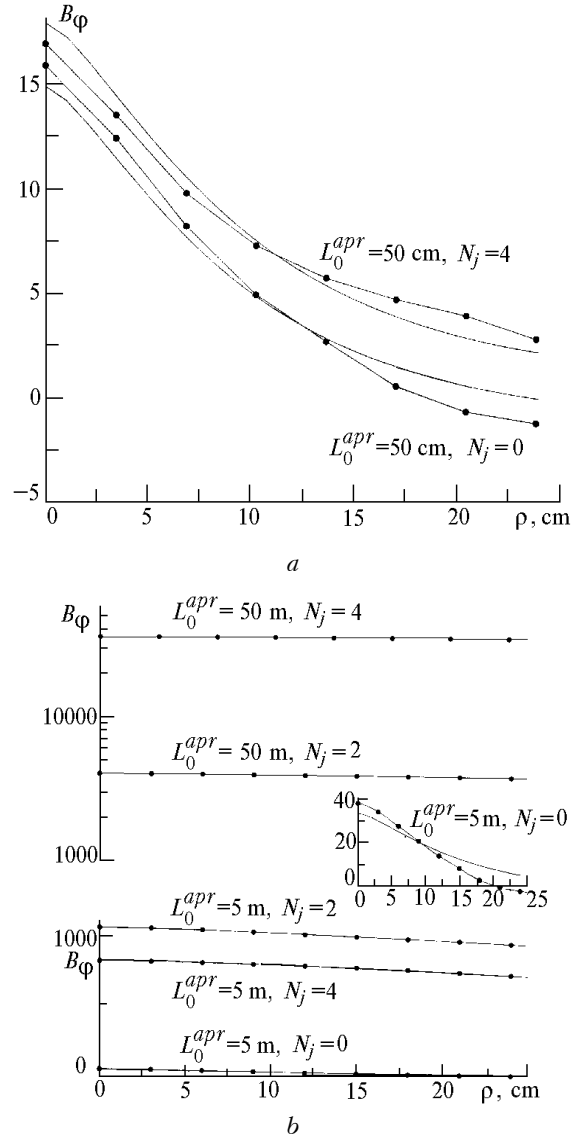


FIG. 1. Correlation function (a, b) of the phase on the screen obtained by the modified subharmonic method at a square  $515 \times 512$  grid of  $51.2 \text{ cm}$  size for Karman spectrum (2) with  $C_n^2 = 5 \cdot 10^{-15} \text{ cm}^{-2/3}$ , a preset outer scale  $L_0^{\text{appr}}$  and number of iterations  $N_j$ ;  $B_{\phi}^{\text{Num}}$  obtained by MCM (—•—);  $B_{\phi}(\rho)$  as approximation by the analytical expression (11) with the parameter  $L_0$  (—).

The Table I presents the values of the outer scale  $L_0$  and the variance  $\sigma_\phi^2$  for a screen formed by the subharmonic method, for different number of iterations  $N_j$  and the turbulence characterized by several *a priori* values of  $L_0^{apr}$  and  $C_n^2 = 5 \cdot 10^{-15} \text{ cm}^{-2/3}$ .

TABLE I.

Number of iterations	<i>A priori</i> values $L_0^{apr} / \sigma_\phi^{2apr}$			
	$N_j$	50 cm/19.6	5 m/907.6	50 m/42126.1
0		44 cm/15.8	71 cm/37.9	71 cm/35.4
2		48 cm/18.2	5.5 m/1055.3	12 m/4066.3
4		46 cm/16.8	4.7 m/815.7	45 m/35865.7

As is seen from the table, the fields obtained by the spectral method  $N_j = 0$  correspond to the set statistics only if the outer scale  $L_0^{apr}$  does not exceed the grid size  $A/2$ . To reproduce larger scales, one should use the subharmonic method. The number of iterations  $N_j$  used increases with increasing outer scale  $L_0^{apr}$ .

#### VARIANCE OF SHIFTS IN THE POSITION OF A COLLIMATED BEAM GRAVITY CENTER UNDER CONDITIONS OF LARGE-SCALE FLUCTUATIONS

The random position of the center of gravity of an optical beam in a plane transversal to the propagation direction is defined by the expression

$$\tilde{\rho}_c^{(i)}(z) = \frac{1}{P_0} \int d^2\rho \rho \tilde{I}^{(i)}(z, \rho), \quad (13)$$

where  $P_0 = \int d^2\rho I(0, \rho)$  is the full power of the beam;

$\tilde{I}^{(i)}(z, \rho)$  is the random intensity distribution over the beam cross section. The variance of the beam shifts  $\sigma_c^2$  was determined as a result of statistical processing of the data array  $\{\tilde{\rho}_c^{(i)}(z), i = 1 \dots M\}$  where  $M$  is the sample size.

The numerical experiment was performed for a collimated Gaussian beam of radius  $a_0 = 2 \text{ cm}$  propagating along a horizontal near-land path of length  $L = 2 \text{ km}$ , the radiation wavelength being  $\lambda = 0.5 \mu\text{m}$ . The parameters of turbulence and calculation grid are presented above, the number of iterations is  $N_j = 4$ . For the considered conditions of the beam propagation, the guaranteed experimental results covered the ranges of both weak and strong turbulent broadening.

A typical sample of the intensity distribution  $\tilde{I}^{(i)}(z, \rho)$  over the beam cross section is presented in Fig. 2 for the distance  $z = 1.5 \text{ km}$ .

The root-mean-square deviation  $\sigma_c$  of the center of gravity of the beam is presented in Fig. 3 as a function of the turbulence parameter  $D_s(2a_0)$ , where  $D_s(2a_0) = 1.1 C_n^2 k^2 L(2a_0)^{5/3}$ . One can see that the beam wandering increases with the increase of the turbulence outer scale  $L_0$ .

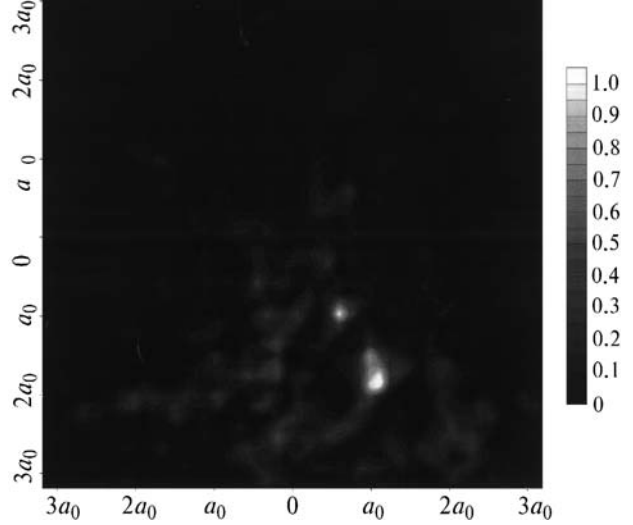


FIG. 2. Typical sample of the intensity distribution  $\tilde{I}^{(i)}(z, \rho)$  over the cross section of a collimated beam with the initial radius  $a_0 = 2 \text{ cm}$ ,  $\lambda = 0.5 \mu\text{m}$ . The beam propagates along a near ground path, the turbulence parameter is  $C_n^2 = 5 \cdot 10^{-15} \text{ cm}^{-2/3}$  for  $z = 1.5 \text{ km}$ .

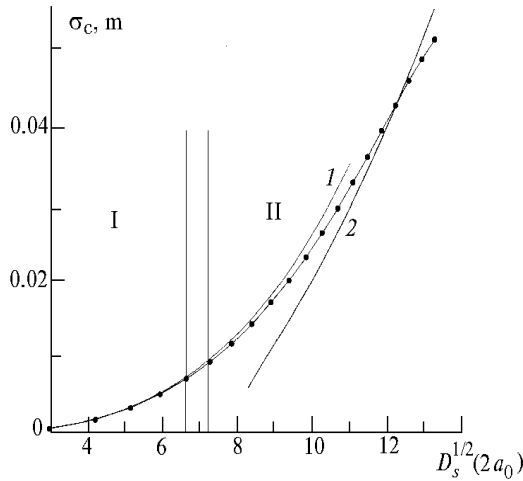
To verify the analytical theories, the results of statistical experiments were compared with the calculations made using phase approximation of the Huygens–Kirchhoff method (PAHKM).<sup>17</sup> Under the conditions

$$0 \leq L/F \leq 1, \quad \Omega \geq 1, \quad (14)$$

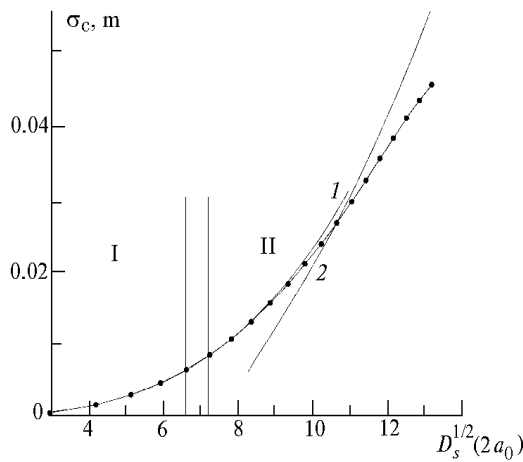
where  $F$  is the focusing radius of the Gaussian beam;  $\Omega = ka_0^2/L$  is the Fresnel number of the transmitting aperture, the approximation yields the following expressions for  $\sigma_c^2$ :

at  $\beta_0^2 \ll \Omega^{1/2}$

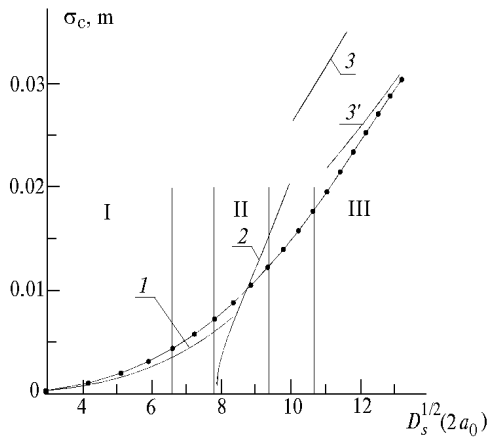
$$\begin{aligned} \sigma_c^2 &= a_0^2 \xi_1(\Omega, L/F, \beta) D_s(2a_0) + \\ &+ a_0^2 \xi_2(\Omega, L/F, \beta) D_s^2(2a_0); \\ \xi_1(\Omega, L/F, \beta) &= 1.17 \Omega^{-2} a_0^{1/3} \times \\ &\times \int_0^1 d\zeta (1-\zeta)^2 \{a_g^{-1/3}(\zeta L) - [a_g^2 + a_0^2 \beta]^{-1/6}\}; \\ a_g(\zeta L) &= \zeta a_0 \Omega^{-1} \left[ 1 + \Omega^2 \zeta^{-2} \left( 1 - \zeta \frac{L}{F} \right)^2 \right]^{1/2}; \\ \xi_2(\Omega, L/F, \beta) &= \\ &= 0.24 \Omega^{-10/3} \int_0^1 d\zeta (1-\zeta)^2 \zeta^{7/3} \left( 1 - \zeta \frac{L}{F} \right)^{-5/3} \times \\ &\times \int_0^1 d\eta (1-\eta)^{10/3} \left( 1 - \zeta \eta \frac{L}{F} \right)^{-5/3}; \end{aligned}$$



a



b



c

FIG. 3. The rms deviations  $\sigma_c$  of the center of gravity as functions of the turbulence parameter  $D_s^{1/2}(2a_0)$  obtained by MCM for a collimated beam with the initial radius  $a_0 = 2$  cm,  $\lambda = 0.5 \mu\text{m}$ . The beam propagated along a near-ground path, the turbulence parameter  $C_n^2 = 5 \cdot 10^{-15} \text{ cm}^{-2/3}$  (curves with dots). The curves 1, 2, and 3 are calculated by Eqs. (15), (16), and (17); the validity domains for the expressions are denoted by Roman figures I, II, and III;  $L_0 = 50$  m (a);  $L_0 = 5$  m (b);  $L_0 = 50$  cm (c).

$$\begin{aligned} \beta_0^2 &= 1.23 C_n^2 k^{7/6} L^{11/6}; \\ \beta &= (0.54L_0)^2 / (2\pi^2 a_0^2), \end{aligned} \quad (15)$$

at  $\Omega^{5/3} \ll D_s(2a_0) \ll \Omega^{5/3}(1 + \beta)^{5/6}$

$$\begin{aligned} \sigma_c^2 &= 1.54 a_0^2 \Omega^{-5/3} D_s^{4/5}(2a_0) - \\ &- 1.79 a_0^2 \Omega^{-11/8} D_s^{5/8}(2a_0), \end{aligned} \quad (16)$$

at  $D_s(2a_0) \gg \Omega^{5/3}(1 + \beta)^{5/6}$

$$\begin{aligned} \sigma_c^2 &= a_0^2 \Omega^{-11/8} D_s^{5/8}(2a_0) 1.79[(1 + \beta)^{7/48} - 1] + \\ &+ a_0^2 \Omega^{-3/2} D_s^{1/2}(2a_0) \{\beta^{-1/6}[(1 + \beta)^{1/12} - 1]/2\}. \end{aligned} \quad (17)$$

The curves 1, 2, and 3 are calculated analytically by formulas (15), (16), and (17); the Roman figures I, II, and III show the domains where the expressions are valid. One can see that the analytical curve coincides with the results of the numerical experiment in the domain I corresponding to weak turbulence. The best coincidence is observed for the outer scale 5 m for which the analytical curve 1 behaves well in the domain II. For  $L_0 = 50$  cm, the applicability criterion (15) becomes incorrect. The discrepancy between the functions obtained analytically and by MCM are observed near the boundary of the domain. In Ref. 18, another estimate of the applicability range is presented by formula

$$D_s(2a_0) \ll \Omega^{4/3} (1 - (1 + \beta)^{-1/6}). \quad (18)$$

In this case, the right-hand side boundary of the domain I corresponds to the value  $D_s(2a_0) \approx 4$ .

The analytical expression (16) for  $\sigma_c^2$  does not depend on the turbulence outer scale what is not confirmed in the numerical experiment. For  $D_s^{1/2}(2a_0) = 9$ , the value  $\sigma_c$  varies from  $1.1 \cdot 10^{-2}$  m ( $L_0 = 50$  cm) to  $1.8 \cdot 10^{-2}$  m ( $L_0 = 50$  cm). The theory predicts a stronger growth of the function  $\sigma_c(D_s^{1/2})$ .

In the domain III, the analytical and numerical values of  $\sigma_c$  differ strongly ( $\approx 40\%$ ). If the outer scale decreases from 50 to 25 cm in Eq. (17), the discrepancy does not exceed 5% (curve 3' in Fig. 3c). This can be explained by the fact that the expression (17) is an asymptotic. With the decrease of  $L_0$ ,  $\beta$  also decreases and, consequently, the inequality defining the applicability of Eq. (17) is fulfilled better.

### FOCUSED BEAM

In the numerical experiment we simulated field investigations of the shift variance and broadening of a laser beam in the turbulent atmosphere.<sup>19</sup> We have considered a strongly focused Gaussian beam of the initial radius  $a_0 = 15.1$  cm. The beam propagated along a path at a height  $H = 2$  m to the distance  $L = F = 1750$  m. The focusing radius was  $1/130$  of the

diffraction length, the wavelength was  $\lambda = 0.63 \mu\text{m}$ . The beam rms shift  $\sigma_c$  and the efficient radius  $a_{\text{eff}}$  were measured at the geometric focus for two values  $C_n^2$  equal to  $3 \cdot 10^{-15} \text{ cm}^{-2/3}$  and  $1.5 \cdot 10^{-14} \text{ cm}^{-2/3}$ . The radius  $a_{\text{eff}}$  in the field experiment was determined as the half width of the beam profile averaged over 100–300 instant responses.

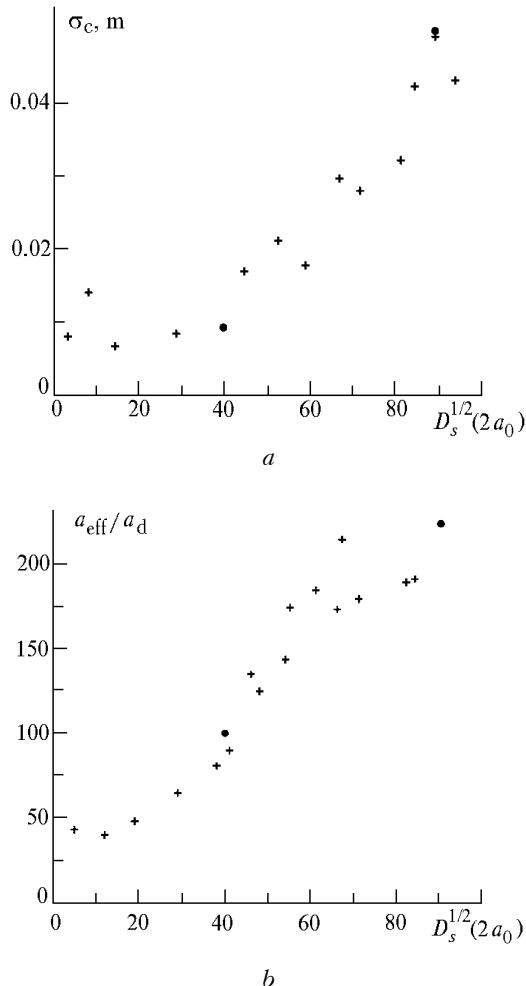


FIG. 4. Numerical MCM simulation of a field experiment<sup>19</sup> for a focused Gaussian beam ( $a_0 = 15.1 \text{ cm}$ ,  $\lambda = 0.63 \mu\text{m}$ ,  $H = 2 \text{ m}$ ,  $L = F = 1750 \text{ m}$ ) for  $C_n^2 = 3 \cdot 10^{-15} \text{ cm}^{-2/3}$  and  $1.5 \cdot 10^{-14} \text{ cm}^{-2/3}$  (dots). The "+" signs denote the data of the field experiment.<sup>19</sup> The rms shift of the beam  $\sigma_c$  (a); the ratio of the efficient radius of the beam  $a_{\text{eff}}$  to its diffraction radius  $a_d$ .

The numerical experiment was performed with  $1024 \times 1024$  grid, in order to guarantee high spatial resolution (the diffraction radius of the beam at the focus is  $a_d = 1.16 \text{ mm}$ ). The phase screens were generated by the modified subharmonic method with the number of iterations  $N_j = 2$ . This number of iterations was sufficient to reproduce the outer scale  $L_0 = 0.4H = 0.8 \text{ m}$  on the grid of size  $A = 1$  with a good accuracy. The path involved 20 screens, the

statistical ensemble consisted of 50 realizations. As is seen from Fig. 4, the numerical results well agree with the data of the field experiment for two strongly different values of the parameter  $D_s(2a_0)$ . This permits one to speak about the reliability of the results obtained by MCM.

## CONCLUSION

We have analyzed the phase screens obtained by the modified subharmonic method. It is demonstrated that two subharmonic iterations are sufficient to reproduce the outer scale of atmospheric turbulence exceeding the size of the numerical grid no more than by 10 times. Four iterations in the subharmonic method make it possible to reproduce the phase screens within good accuracy for turbulence with the outer scale exceeding the grid size by 100 times.

In the range of weak turbulent broadening (15), analytical estimates of the shift variance for the center of gravity of the beam coincide with the results of statistical experiments for large values of the outer scale  $L_0 = 5 \text{ m}$  and significantly differ for  $L_0 = 50 \text{ m}$ .

In contrast to analytical calculations in PAHKM, numerical experiments in the range of strong turbulent broadening (16) demonstrate significant dependence of the shift variance of the beam center gravity on the outer scale. For the turbulence outer scales 50 cm and 50 m, the variance values differ by 60%. In the range (17), to agree with the analytical data, the strong inequality must be fulfilled with a reserve of two orders.

Statistical simulation of one of the field experiments<sup>19</sup> shows a good agreement between the numerical and experimental values of the shift variance and efficient size of the beam.

## ACKNOWLEDGMENT

The work was partially supported by Samsung Electronics, SSM program.

## REFERENCES

1. V.P. Kandidov, Usp. Fiz. Nauk **166**, No. 12, 1309–1338 (1996).
2. J.M. Martin and S.M. Flatte, Appl. Opt. **27**, No. 11, 2111–2126 (1988).
3. R. Dashen, G.Yu. Wang, S.M. Flatte, and C. Bracher, J. Opt. Soc. Am. A. **10**, No. 6, 1233–1242 (1993).
4. V.P. Kandidov, M.P. Tamarov, and S.A. Shlyonov, Atmos. Oceanic Opt. **9**, No. 11, 916–920 (1996).
5. V.P. Kandidov, Izv. Akad. Nauk SSSR, Fiz. **49**, No. 3, 24–31 (1985).
6. V.E. Zuev, P.A. Konyaev, and V.P. Lukin, Izv. Vyssh. Uchebn. Zaved., Ser. Fizika **28**, No. 11, 6 (1985).
7. V.A. Vysloukh, V.P. Kandidov, S.S. Chesnokov, and S.A. Shlyonov, Izv. Vyssh. Uchebn. Zaved., Ser. Fizika **28**, No. 11, 30 (1985).

8. Fr.G. Gebhardt, Proc. SPIE **2120**, 76 (1994).
9. J.A. Fleck, J.R. Morris, and M.D. Feit, Appl. Phys. **10**, 129 (1976).
10. V.P. Kandidov and V.I. Ledenev, Vestn. Mosk. Univ., Fiz. Astron. **23**, 3 (1982).
11. R.J. Noll, J. Opt. Soc. Am. **66**, 207 (1976).
12. V.P. Kandidov and S.A. Shlyonov, in: *Techn. Program of Eighth Laser Optics Conference* (St. Petersburg, 1995), p. 48.
13. V.P. Lukin, B.V. Fortes, and P.A. Konyaev, Proc. SPIE **2222**, 522 (1994).
14. B.J. Herman and L.A. Strugala, Proc. SPIE **1221**, 183–192 (1990).
15. R.G. Lane, A. Glindemann, J.C. Dainty, Waves in Random Media **2**, No. 3, 209–224 (1992).
16. E.M. Johanson and D.T. Gavel, Proc. SPIE **2200**, 372–383 (1994).
17. V.L. Mironov, *Laser Beam Propagation in a Turbulent Atmosphere* (Nauka, Novosibirsk, 1981), 246 pp.
18. V.E. Zuev, V.A. Banakh, and V.V. Pokasov, *Optics of Turbulent Atmosphere* (Gidrometeoizdat, Leningrad, 1988), 270 pp.
19. M.A. Kallistratova and V.V. Pokasov, Izv. Vyssh. Uchebn. Zaved., Ser. Radiofiz. **14**, No. 8, 1200–1207 (1971).